

# High-power linearly-polarized single-frequency thulium-doped fiber master-oscillator power-amplifier

L. Pearson, J. W. Kim\*, Z. Zhang, M. Ibsen, J. K. Sahu, and W. A. Clarkson

*Optoelectronics Research Centre, University of Southampton, Southampton, SO17 1BJ, UK*

*\*jwk@orc.soton.ac.uk*

**Abstract:** We report a high power narrow-linewidth source at  $\sim 2\ \mu\text{m}$  based on a Tm-doped fiber distributed-feedback master-oscillator and three Tm fiber amplifier stages. The master-oscillator and first two amplifier stages were in-band pumped by Er,Yb fiber lasers operating at 1565 nm, and the final stage amplifier was cladding-pumped at 795 nm by two spatially-combined diode-stacks. The MOPA yielded 100 W of single frequency output at 1943 nm with a beam propagation factor ( $M^2$ ) of 1.25 and with a polarization extinction ratio of  $>94\%$ . The output power was limited by thermally-induced damage in the final amplifier stage. The prospects for further power scaling are considered.

©2010 Optical Society of America

**OCIS codes:** (140.0140) Lasers and laser optics; (140.3070) Infrared and far infrared lasers; (140.3280) Laser amplifiers; (140.3510) Lasers, fiber; (140.3570) Lasers, single-mode

---

## References and links

1. T. F. Morse, K. Oh, and L. J. Reinhart, "Carbon dioxide detection using a co-doped Tm-Ho optical fiber," *Proc. SPIE* **2510**, 158–164 (1995).
2. S. W. Henderson, P. J. M. Suni, C. P. Hale, S. M. Hannon, J. R. Magee, D. L. Bruns, and E. H. Yuen, "Coherent laser radar at  $2\ \mu\text{m}$  using solid-state lasers," *IEEE Trans. Geosci. Rem. Sens.* **31**(1), 4–15 (1993).
3. W. A. Clarkson, N. P. Barnes, P. W. Turner, J. Nilsson, and D. C. Hanna, "High-power cladding-pumped Tm-doped silica fiber laser with wavelength tuning from 1860 to 2090 nm," *Opt. Lett.* **27**(22), 1989–1991 (2002).
4. D. Y. Shen, J. K. Sahu, and W. A. Clarkson, "High-power widely tunable Tm: fibre lasers pumped by an Er, Yb co-doped fibre laser at  $1.6\ \mu\text{m}$ ," *Opt. Express* **14**(13), 6084–6090 (2006).
5. G. D. Goodno, L. D. Book, and J. E. Rothenberg, "Low-phase-noise, single-frequency, single-mode 608 W thulium fiber amplifier," *Opt. Lett.* **34**(8), 1204–1206 (2009).
6. Z. Zhang, D. Y. Shen, A. J. Boyland, J. K. Sahu, W. A. Clarkson, and M. Ibsen, "High-power Tm-doped fiber distributed-feedback laser at 1943 nm," *Opt. Lett.* **33**(18), 2059–2061 (2008).
7. J. Geng, J. Wu, S. Jiang, and J. Yu, "Efficient operation of diode-pumped single-frequency thulium-doped fiber lasers near  $2\ \mu\text{m}$ ," *Opt. Lett.* **32**(4), 355–357 (2007).
8. N. Y. Voo, J. K. Sahu, and M. Ibsen, "345 mW 1836 nm single frequency DFB fiber laser MOPA," *IEEE Photon. Technol. Lett.* **17**(12), 2550–2552 (2005).
9. S. D. Jackson, and S. Mossman, "Efficiency dependence on the  $\text{Tm}^{3+}$  and  $\text{Al}^{3+}$  concentrations for  $\text{Tm}^{3+}$ -doped silica double-clad fiber lasers," *Appl. Opt.* **42**(15), 2702–2707 (2003).
10. J. W. Kim, D. Y. Shen, J. K. Sahu, and W. A. Clarkson, "Fiber-Laser-Pumped Er:YAG Lasers," *IEEE J. Sel. Top. Quantum Electron.* **15**(2), 361–371 (2009).
11. P. F. Moulton, G. A. Rines, E. Slobodtchikov, K. F. Wall, G. Frith, and B. Samso, A. Carter, "Tm-doped fiber lasers: Fundamentals and power scaling," *IEEE J. Sel. Top. Quantum Electron.* **15**(1), 85–92 (2009).

---

## 1. Introduction

In recent years there has been growing interest in high power laser sources operating in the eyesafe wavelength regime around two-microns driven by a range of applications, including spectroscopy, gas sensing, LIDAR, materials processing and various defence-related applications. Two-micron lasers also provide the ideal starting point for nonlinear frequency conversion to the mid-infrared wavelength region [1,2]. For some of these applications, the requirement for high output power and good beam quality is accompanied by the need for flexibility in operating wavelength and a narrow-linewidth, linearly-polarized output. One promising route to these performance specifications is via the use of a master-oscillator

power-amplifier (MOPA) configuration based on a single-frequency seed laser and a high-power cladding-pumped Tm-doped multi-stage fiber amplifier. Fibers benefit from a geometry that allows simple thermal management and offer a high degree of immunity from the effects of heat loading that are often so detrimental to the performance of conventional crystal-based solid-state lasers. Moreover, Tm-doped silica fiber offers a very broad transition linewidth on the  $^3F_4 - ^3H_6$  transition allowing operation at any wavelength in the 1.7–2.1  $\mu\text{m}$  band [3,4]. In recent work, Goodno et al. [5] reported a MOPA based on a single-frequency diode laser, a three-stage polarization-maintaining (PM) Tm fiber pre-amplifier and a final (non-PM) power-amplifier stage with >600 W of narrow-linewidth output at 2040 nm. In this paper we report a Tm fiber MOPA system based only on Tm-doped fiber gain elements and with a polarization-maintaining cladding-pumped final amplifier stage that yields 100 W of linearly-polarized single-frequency output at 1943 nm, limited by thermally-induced damage.

## 2. Experimental set-up

The MOPA configuration used in our experiments is shown in Fig. 1 and comprised a narrow-linewidth Tm-doped fiber distributed-feedback (DFB) laser, followed by two intermediate Tm fiber pre-amplifier stages and then a final cladding-pumped PM Tm fiber power amplifier stage. An important element of the MOPA design is the choice of single-frequency seed laser since this influences the design and number of fiber amplifier stages required to reach a given power level. Tm-doped fiber DFB lasers have the potential to be scaled to be to significantly higher output power than can typically be achieved from other types of monolithic seed laser operating in the two-micron wavelength regime [6–8] and hence offer the prospect of a simpler MOPA system with fewer amplifier stages and intermediate components (e.g. isolators). A further attraction is compatibility with fiber amplifiers and fiberized components allowing for simpler integration and, ultimately, an all-fiber design.

A key element of the DFB laser design is the Tm fiber core composition which must be sufficiently photosensitive to UV writing of the DFB grating structure and must allow efficient absorption of pump light in a relatively short fiber device length (typically < 10 cm). The Tm-doped fiber used for the DFB master-oscillator was fabricated in-house via modified chemical vapor deposition (MCVD) and solution doping. The resulting fiber had a Tm and Ge co-doped alumino-silicate core with a diameter of  $\sim 10 \mu\text{m}$  and a numerical aperture (NA) of 0.17, surrounded by a pure silica circular cladding with a diameter of 125  $\mu\text{m}$ . Direct diode pumping of the  $^3H_6 - ^3H_4$  transition is not attractive for core-pumped Tm DFB fiber lasers due to the relatively low brightness of commercially available pump diodes at  $\sim 790 \text{ nm}$ . For this reason, pump light for the DFB laser was provided by a 10 W single-mode Er,Yb co-doped fiber laser with a linewidth of <2 nm (FWHM) and with operating wavelength (1565 nm) selected for efficient in-band pumping of the  $^3H_6 - ^3F_4$  transition in Tm-doped silica glass. This pumping scheme has the attraction of relatively low quantum defect heating (<20%) in the Tm fiber and hence offers the potential for scaling DFB laser powers to the multi-watt regime. A relatively high Tm concentration ( $\sim 1 \text{ wt.}\%$ ) was employed in the fiber to yield a high small signal absorption coefficient in the core of  $\sim 100 \text{ dB/m}$  at the pump wavelength of 1565 nm and hence allow efficient pumping of the short fiber device lengths that are required for DFB laser configurations. To facilitate writing of a high reflectivity grating, the core photosensitivity was enhanced by hydrogen-loading. The DFB grating produced was 8 cm long with a  $\pi$ -phase shift 6 mm from the grating's mid-point in order to produce a predominantly single-ended output. The grating pitch was selected for laser operation at 1943 nm and the grating had a measured coupling coefficient  $\kappa$  of  $\sim 100 \text{ m}^{-1}$ . The output beam propagation ( $M^2$ ) for the Er,Yb fiber pump laser was measured to be <1.1 allowing efficient coupling of pump light into the DFB fiber via a length of standard single-mode passive fiber

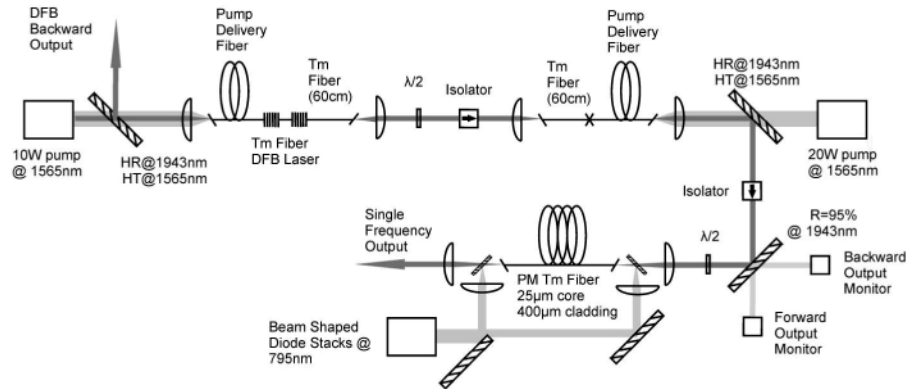


Fig. 1. Schematic diagram of Tm fiber master-oscillator power-amplifier.

(core diameter 9  $\mu\text{m}$  and NA of 0.14) spliced directly to the DFB laser. The coupling efficiency for pump light into the DFB laser was estimated to be 80%.

The DFB laser yielded a maximum forward output power of 875 mW at 1943 nm for a launched pump power of 8.1 W corresponding to 3.1 W of absorbed power. The backward propagating beam was extracted with the aid of a dichroic mirror and had a maximum power of only 70 mW, confirming predominantly single-ended operation. The residual pump power (i.e. 5 W) was used to pump a simple first-stage Tm fiber amplifier comprising 60 cm of the same Tm fiber spliced directly to the DFB fiber without the need of an intermediate isolator with an angle-polished output facet to suppress broadband feedback. The DFB laser and first-stage amplifier together yielded a maximum output power of 3.1 W in a beam with  $M^2 < 1.06$ . The output from the DFB master-oscillator consisted of two orthogonally-polarized modes with a frequency spacing of 660 MHz due to residual birefringence in the fiber [6]. Operation on a single linearly-polarized mode can in principle be achieved using a fiber design with higher photosensitivity to allow the writing of a grating with a polarization-dependent reflectivity. In this preliminary design, selection of a single (linearly-polarised) axial mode was achieved with the aid of a half-wave plate and a polarizer. The latter forming part of an isolator with measured isolation of 16.9 dB at 1943 nm inserted between the first and second stage to prevent parasitic lasing or the build-up of amplifier spontaneous emission in the amplifier chain. Single frequency operation from the output was confirmed by a scanning Fabry Perot interferometer with a Free-Spectral-Range (FSR) of 6 GHz and a finesse of 103 [6].

The second-stage Tm fiber amplifier also comprised a 60 cm long section of the same Tm-doped fiber as used in the DFB laser followed by a short length of standard single mode delivery spliced directly to the Tm fiber. Signal light after the first-stage amplifier and isolator was launched into the second-stage amplifier stage with a launched efficiency of 75% corresponding to  $\sim 1$  W of launched signal power. Pump light for the second-stage amplifier was provided by an Er,Yb co-doped fiber laser with a maximum output power of 20 W at 1565 nm. The latter was free-space coupled into the delivery fiber with a launching efficiency of 80% using a dichroic mirror to extract the amplified signal light (Fig. 1). Both end facets of the fibers were angle-polished to  $\sim 10^\circ$  to suppress parasitic lasing. Under these operating conditions, the second-stage amplifier produced a maximum amplified signal power of 10 W for 16 W of launched pump power, corresponding to a slope efficiency of  $\sim 63\%$  (Fig. 2). A double-clad polarization-maintaining (PM) large-mode-area Tm-doped fiber supplied by Nufern (PLMA-TDF-25F/400) was employed in the final power amplifier stage. This fiber had a Tm-doped alumino-silicate core with a high Tm concentration to promote the ‘two-for-one’ cross-relaxation process ( ${}^3\text{H}_4 + {}^3\text{H}_6 \rightarrow {}^3\text{F}_4 + {}^3\text{F}_4$ ) [9] and hence enhance the overall efficiency. The core had a diameter of 25  $\mu\text{m}$  with a raised refractive index pedestal to reduce

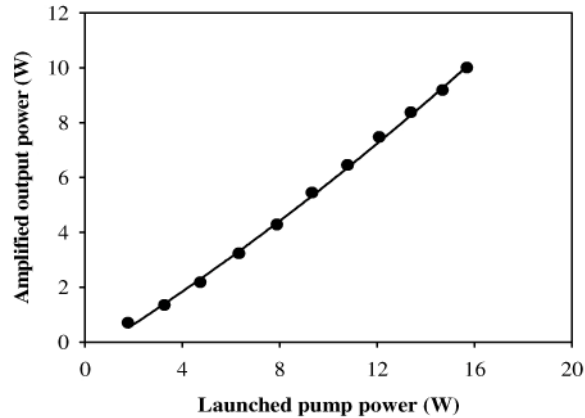


Fig. 2. Signal output power as a function of launched pump power for the intermediate amplifier.

the core numerical aperture to  $\sim 0.1$  and a pure silica inner-cladding of diameter,  $400\ \mu\text{m}$  with stress-rods to produce a linear birefringence of  $2 \times 10^{-4}$ . The latter was surrounded with a low refractive index polymer coating to yield a high numerical aperture (0.4 NA) for the inner-cladding pump guide. The effective absorption coefficient for pump light at  $795\ \text{nm}$  launched into the inner-cladding was measured via the cut-back technique to be  $\sim 4.5\ \text{dB/m}$ , so a fiber length of  $\sim 4\ \text{m}$  was selected for the amplifier. Both ends of the fiber were angle-polished at  $\sim 10^\circ$  to suppress broadband feedback. Pump light at  $\sim 795\ \text{nm}$  was provided by two six-bar diode-stacks. After fast-axis collimation with an array of high numerical aperture cylindrical microlenses, each stack had a fill-factor in the fast direction of  $< 50\%$ . Their output beams were then spatially-multiplexed using a simple slotted-mirror beam-combiner to effectively remove the 'dead-space' between adjacent bars and allow any beam pointing errors to be corrected. The combined output beam had beam propagation factors,  $M_x^2 < 600$  parallel to the diode-bar (slow direction) and  $M_y^2 < 60$  in the orthogonal (fast) direction, and a polarization extinction ratio (PER) of  $> 98\%$ . Further conditioning of the pump beam was achieved by splitting the combined beam in the slow direction using a knife-edge mirror and then polarization-combining the two beams to achieve a further reduction in  $M_x^2$  by roughly a factor-of-two. The resulting beam was then split again in the slow direction to yield two pump beams of roughly equal power and with  $M^2$  parameters,  $M_x^2 \approx 175$  and  $M_y^2 \approx 65$  to allow pumping of both ends of the Tm fiber. This arrangement has the attraction over single-end pumping that higher pump launch efficiency can be achieved and thermal loading is more evenly distributed along the fiber reducing the risk of thermally-induced damage. Pump light was coupled into both ends of the Tm fiber with the aid of dichroic mirrors with reflectivity  $> 98\%$  at the pump wavelength at  $45^\circ$  and high transmission ( $> 97\%$ ) at the signal wavelength ( $1943\ \text{nm}$ ) to simultaneously allow pump launching and extraction of the signal (Fig. 1). Using this pumping arrangement we could launch  $> 83\%$  of the incident pump light into the Tm fiber and the maximum pump power available was  $430\ \text{W}$ . Both end sections of the fiber were mounted in water-cooled V-groove heat-sinks to reduce the risk of thermally-induced damage to the fiber coating due to the unlaunched pump power. The remaining central portion of the fiber was air-cooled by an arrangement of fans to facilitate heat removal.

The output from the second amplifier was collimated with the aid of an aspheric lens of focal length,  $8\ \text{mm}$ , to achieve a beam diameter of  $\sim 2.5\ \text{mm}$  and was then coupled into the final amplifier stage via an arrangement comprising a pair of beam steering mirrors, an isolator and a half-wave plate. The latter was used to align the polarization direction of the signal to be parallel to the slow axis of the PM Tm-doped fiber. The isolator had a CW damage threshold of  $200\ \text{W/cm}^2$ , so, in order to reduce the risk of damage to the isolator and avoid degradation in beam quality due to thermally-induced beam distortion in the isolator, the output power from the second-stage amplifier was limited to  $< 5\ \text{W}$ . The isolator optics

had a combined loss (i.e. due to absorption in the Faraday rotator and imperfect antireflection coatings) of approximately 15%. The transmitted signal beam had a measured beam propagation factor ( $M^2$ ) of  $<1.07$ , confirming that thermally-induced beam distortion was negligible at this power level. The signal beam was then launched into the final-stage amplifier with a measured coupling efficiency of 75% resulting in a maximum launched signal power of  $\sim 3$  W. Due to the slightly multimode nature of the core, care was taken to match the launched signal beam diameter to the fundamental mode diameter of  $21 \mu\text{m}$  to minimize higher order mode content. One of the beam steering mirrors had a transmission of 5%, and hence allowed the simultaneous monitoring of the input signal to the final amplifier and any backward propagating output due to parasitic lasing or stimulated Brillouin scattering (SBS).

### 3. Results and discussion

The output power from the final-stage amplifier as a function of launched pump power is shown in Fig. 3. The amplifier yielded a maximum output power of  $\sim 100$  W for a combined launched pump power of 190 W limited by thermally-induced damage. The slope efficiency with respect to launched pump power was  $\sim 59\%$  indicating that the pumping quantum efficiency is  $>1.44$ . Single-frequency operation was maintained up to the maximum output power and was confirmed with the aid of a scanning Fabry Perot interferometer with FSR of 6 GHz and a finesse of 103. The backward propagating output power as a function of pump power is also shown in Fig. 3. The power in the backward propagating beam did not exceed 20 mW and hence there was no evidence of SBS or parasitic lasing. Moreover, the amplified spontaneous emission content of the output was negligible. The amplifier yielded a nearly diffraction-limited single-mode output beam with a measured  $M^2$  parameter of 1.25 at all power levels. The slightly degraded nature of the output beam can be attributed to phase aberration that results from the input and output dichroic mirrors inclined at  $45^\circ$  to the single beam path at the input end and output end of the amplifier. Thus, the use of near normal incidence dichroic mirrors or, alternatively, an all-fiber pump coupling scheme to avoid the need for dichroic mirrors should improve the output beam quality. The PER was measured to be  $>94\%$  confirming predominantly linearly-polarized nature of the output beam.

The main factor limiting the output power from the MOPA was thermally-induced degradation of the fiber's polymer outer-coating and consequent damage to the fiber in the final amplifier stage. In most designs of double-clad fiber, the outer-coating serves both as a protective layer and as the low index layer allowing pump light to be guided in the inner-

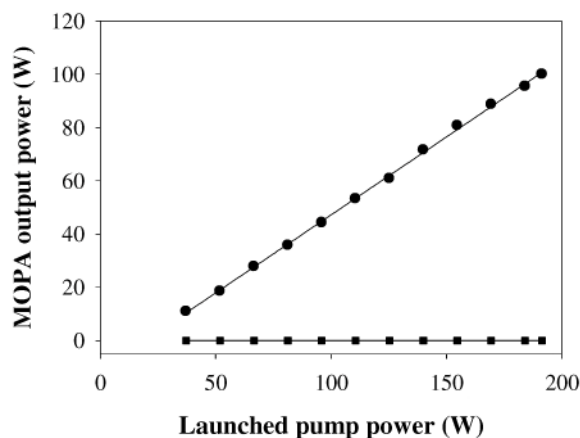


Fig. 3. The MOPA output power (circle) and the backward propagating power (square) as a function of launched pump power.

cladding pump guide. Usually, as is the case here, the outer-coating is a low refractive index fluorinated polymer that can withstand temperatures up to  $\sim 150^\circ\text{C}$  before the onset of damage. The upper limit on the heat deposition density in the core,  $P_{hmax}$  that can be tolerated before coating damage can be estimated from the following Eq. (1) [10]:

$$P_{hmax} \approx 4\pi(T_d - T_s) \left[ \frac{2}{K_{oc}} \log_e \left( \frac{r_{oc}}{r_{ic}} \right) + \frac{2}{r_{oc}h} \right]^{-1} \quad (1)$$

where  $T_d$  is the maximum temperature that the coating can tolerate,  $T_s$  is the temperature of the surroundings (or heat-sink),  $K_{oc}$  is the thermal conductivity of the outer-coating,  $r_{oc}$  is the radius of the outer-coating,  $r_{ic}$  is the radius of the inner-cladding and  $h$  is the heat transfer coefficient. Figure 4 shows  $P_{hmax}$  as a function of  $h$  for the fiber used in the final amplifier stage. With our present configuration the value for  $P_{hmax}$  at which damage occurs is around  $40 \text{ Wm}^{-1}$  implying that the heat transfer coefficient is  $\sim 200 \text{ Wm}^{-2}\text{K}^{-1}$ . The problem of coating damage is particularly acute in cladding-pumped Tm fiber sources because of the high pump deposition density that results from the use of high Tm concentrations as required for enhancing efficiency via the ‘two-for-one’ cross-relaxation process. Clearly, a more effective heat-sinking arrangement to increase the heat transfer coefficient, for example water-cooling of the active fiber [11], could yield an order-of-magnitude increase in the thermal-limit on output power opening up the prospect of output power in the kilowatt regime, subject to effective suppression of SBS. It is worth noting that the use of an improved outer-coating material with higher thermal conductivity and a higher damage limit could dramatically improve the thermal handling limit of Tm fiber sources benefiting a range of applications for two-micron radiation.

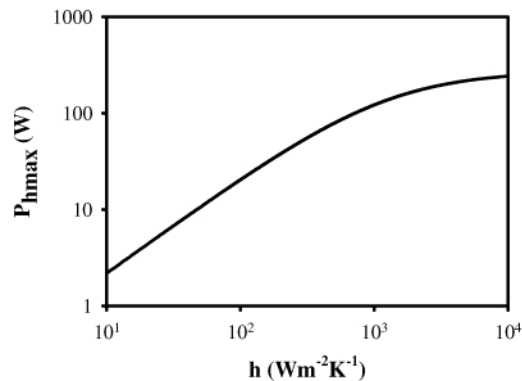


Fig. 4. Upper limit on the heat deposition density in the core,  $P_{hmax}$  versus heat transfer coefficient.

#### 4. Conclusions

We have demonstrated a 100 W single-frequency Tm fibre master-oscillator power-amplifier with a linearly-polarized, near-diffraction-limited output at 1943 nm. The slope efficiency for the final amplifier stage was 59% with respect to launched power. The maximum output power was limited by thermally-induced degradation of the coating. More aggressive thermal management in combination with the use of a better optimized outer-coating should yield an improvement in thermal handling opening up the prospect of single-frequency Tm fiber MOPA power in the kilowatt regime.

#### Acknowledgements

This work was supported by the European Commission under the Information Society Technologies priority of the Sixth Framework Program through contract FP6/IST/34010 and by the Engineering and Physical Sciences Research Council.